The fine structure of cyclotron and spin resonances at their crossing: interplay between spin-orbit and Coulomb interactions

1993 J. Phys.: Condens. Matter 5 8725

(http://iopscience.iop.org/0953-8984/5/46/010)

J. Phys.: Condens. Matter 5 (1993) 8725–8740. Printed in the UK

The fine structure of cyclotron and spin resonances at their crossing: interplay between spin–orbit and Coulomb interactions

Vladimir I Fal'ko†

Max-Planck-Institut für Festkörperforschung, Heisenbergstrasse 1, 70569 Stuttgart, Federal Republic of Germany

Received 29 July 1993

Abstract. We compare the anticrossing of the spin and cyclotron resonances in spin-polarized and non-polarized phases of a two-dimensional electron gas subjected to a strong tilted magnetic field. The spin–orbit coupling splits these resonances into three lines with the gaps between them exactly equal to $\delta_{2n+1} = v_{so}p_F$ and $\delta_{2n} = v_{so}p_F/\sqrt{2}$ at odd- and even-integer factors, respectively. The $1/\sqrt{2}$ factor difference between the gaps δ_{2n} and δ_{2n+1} arises from the existence of two collective spin-wave-density modes in the polarized phase of interacting electrons in the system with two filled Landau levels. This allows us to predict a new type of spectral Shubnikov–de Haas oscillations, which indicates the re-entrance of the system into the spin-polarized state.

1. Introduction

One of the consequences of the general Kohn and Larmor theorems is that the frequencies of the cyclotron (CR) and spin (SR) resonances in a system of two-dimensional (2D) electrons with a parabolic dispersion is not affected by the electron–electron interaction and, therefore, are insensitive to the phase transitions into various collective states formed by the direct or exchange Coulomb effects [1–6]. This statement is exact and was proved to be valid for the Wigner crystalline phase of 2D electrons, as well as for any liquid (compressible or incompressible, spin-polarized or non-polarized) phase.

On the other hand, the deviations of the electron dispersion law from parabolicity makes it possible to display the efficiency of the Coulomb correlation effects in the spectral position and fine structure of resonances [7–9]. Among the sources of non-parabolicity, the spin–orbit coupling is one of the most interesting, but usually it is too weak to produce effects that are spectroscopically observable. Nevertheless, the weakness of the spin–orbit coupling can be partly compensated for in the case of the degeneracy of spin-split Landau levels, $(n, \uparrow)$ and $(n+1, \downarrow)$, when it mixes the states with equal energies [10]. As well as spin- and inter-Landau-level energy splitting being coincident with the frequencies of the spin and cyclotron resonances, this physical situation corresponds to that of the SR and CR crossing. The possibility of setting up crossing conditions is one of the features of 2D systems. This can be realized by subjecting the electron gas to a sufficiently tilted magnetic field, so that the strong tilting makes up for the relative smallness of the Zeeman spin splitting [11–13],

† On leave from Theory Department, Institute of Solid State Physics, Russian Academy of Sciences, Chernogolovka, Moscow District, 142432, Russia.

0953-8984/93/468725+16$07.50

$\omega_c = eH_z/mc \simeq \omega_s = \mu g H/\hbar$ †, and two neighbouring Landau levels with different spins have coincident energies. Due to the spin–orbit coupling, the CR acquires some fine structure at this crossing which will be the subject of the analysis below, in particular from the point of view of its sensitivity to the electron–electron correlations.

One of the important consequences of the Coulomb interaction in this system consists in the transition to a collective spin-polarized state near the spin-split Landau level crossing at even-integer filling factors $\nu = 2n$ predicted by Guiliani and Quinn [11] and, probably, observed by Koch *et al* [13] in $In_xGa_{1-x}As$–InP heterostructures. The exchange interaction of the electrons from nearly degenerate levels with those from the lower levels stimulates the spin alignment, so that the electron gas at the CR–SR crossing point has to be already polarized. As shown in section 4, the occupation of two excess Landau levels with the same spins produces a new spin-density wave mode which cannot manifest itself in ordinary spin resonance absorption, but affects the fine structure of CR at its crossing with SR, so that we can predict how it can be indirectly observed [14]. This conclusion comes from a comparison between CR fine structures one can expect in the spin-polarized and non-polarized states of 2D electrons, as discussed in sections 5 and 3, respectively.

The analysis below is based on the approach of inter-Landau-level (magneto) excitons [3, 5, 15]. This approach (see section 2) is applicable to completely filled 2D Landau levels (i.e. to the integer quantum Hall effect conditions) and, formally, requires that the planar cyclotron energy $\hbar\omega_c$ be larger than the Coulomb energy $e^2/\chi\lambda_H$ at the scale of the magnetic length

$$\lambda_H = (\hbar c/eH_z)^{1/2}$$

(where χ is the effective dielectric constant). This allows us to treat both the electron–electron interaction and the spin–orbit coupling as perturbations, but we pay a price: to satisfy the perturbation theory conditions, the g-factor should not be too small, and the calculations below are applicable to heterostructures of materials with a narrow gap (InP, InAs) rather than to GaAs/AlGaAs heterostructures.

As to the spin–orbit coupling in a 2D electron gas, the necessary information about the effective secondary quantized Hamiltonian describing the resonant spin–orbit splitting of degenerate Landau levels is given in appendix A. Appendix B is devoted to an analysis of the competition between the exchange Coulomb interaction and the spin–orbit coupling in the ground-state formation of a gas under artificial degeneracy conditions.

2. Method of inter-Landau-level excitons

Collective excitations in 2D electron systems will be described using the approach of magneto-excitons at completely occupied Landau levels [3, 5, 15]. This approach is based on the fact that at integer filling factors the electrons from filled Landau levels and the positive background of donors form a homogeneous neutral system [16]. In such a case the chargeless excitations from the ground state $|0\rangle$ can be classified by their momenta Q and, before we account for the spin–orbital interaction, also by the projection of the spin S on the direction of a tilted magnetic field. This provides a formal basis $\{\hat{\Psi}^+_{NN'}(Q)|0\rangle\}$ of low-lying excited states in the gas which are composed of an electron taken from the

† We analyse the problem as if $g > 0$. To get the results for a negative g factor one should exchange the spins in each pair of degenerate Landau levels.

$N' = (n', \alpha')$ level and put onto the level $N = (n, \alpha)$ ($\alpha = \downarrow$ or $\uparrow$). These states can be produced from the ground state by means of creation operators $\hat{\Psi}^+_{NN'}(\boldsymbol{Q})$ defined as

$$\hat{\Psi}^+_{NN'}(\boldsymbol{Q}) = \sum_p e^{ipQ_y} a^+_{Np} a_{N'p-Q_x}. \tag{1}$$

Together with the annihilation operators $\hat{\Psi}_{NN'}(\boldsymbol{Q})$,

$$\hat{\Psi}_{NN'}(\boldsymbol{Q}) = e^{-iQ_xQ_y}\hat{\Psi}^+_{N'N}(-\boldsymbol{Q})$$

they make the algebra†

$$[\hat{\Psi}^+_{N_1N_1'}(\boldsymbol{Q}'), \hat{\Psi}_{N_2N_2'}(\boldsymbol{Q})] = e^{-iQ_{1x}Q_{2y}}\delta_{N_2N_1'}\hat{\Psi}^+_{N_1N_2'}(\boldsymbol{Q}+\boldsymbol{Q}') - e^{-iQ_{2x}Q_{1y}}\delta_{N_1N_2'}\hat{\Psi}^+_{N_2N_1'}(\boldsymbol{Q}+\boldsymbol{Q}').$$

In defining the operators in (1) we use the gauge

$$\boldsymbol{A} = (-H_z y + H_y z, -H_x z, 0)$$

and single-electron wavefunctions of the form

$$\psi^{\alpha}_{np} = e^{ipx\lambda_H} H_n(y\lambda_H^{-1} - p)\exp\left(-\frac{(y\lambda_H^{-1} - p)^2}{2}\right)$$

where H_n are normalized Hermitian polynomials and

$$\lambda_H = (\hbar c/eH_z)^{1/2}$$

is the magnetic length determined by the perpendicular to the plane magnetic field component. We also use the dimensionless momenta Q and p measured in the units λ_H^{-1}.

It is convenient to apply a formal representation of inter-Landau-level excitons to the problem of real excitations hybridized by the Coulomb interaction and mixed by the spin–orbit coupling. If we assume that the single-particle energy spacing $\hbar\omega_c \sim \hbar\omega_s$ is much greater than both the Coulomb and spin–orbit energies, the hybridization and mixing involve only several magneto-excitons with close single-particle energies. Hence, in analysing the low-lying excitation spectrum, we can cut the basis of states $\{\hat{\Psi}^+_{NN'}(\boldsymbol{Q})|0\rangle\}$ and work only with those that are in mutual resonance:

$$\epsilon_N - \epsilon_{N'} \simeq \hbar\omega_c.$$

This allows us to replace the full exact many-body Hamiltonian of 2D electrons

$$\hat{H} = \hat{H}_0 + \hat{U} + \hat{V}_{so}$$

by a set of finite-size matrices

$$H_{(\tilde{N},\tilde{N}')(NN')}(\boldsymbol{Q}) = \langle 0|\hat{\Psi}_{\tilde{N}\tilde{N}'}(\boldsymbol{Q})\hat{H}\hat{\Psi}^+_{NN'}(\boldsymbol{Q})|0\rangle - \delta_{N\tilde{N}}\delta_{N'\tilde{N}'}\langle 0|\hat{H}|0\rangle \tag{2}$$

each acting in its own subspace of excitonic states with a fixed 2D momentum $\boldsymbol{Q}$ and possible projections $S = 0, \pm 1$ of a spin to the axis $\boldsymbol{h} = \boldsymbol{H}/H$. In these equations the pairs of Landau level numbers (N, N') and $(\tilde{N}, \tilde{N}')$ serve as indices of these matrices and,

† Here and everywhere below we omit the insufficient normalization factor from the intermediate formulae.

generally, each matrix has a block-diagonal form with off-diagonal elements describing the conversion of one of the excitations $\Psi^+_{NN'}(Q)|0\rangle$ into another $\Psi^+_{\bar{N}\bar{N}'}(Q)|0\rangle$ in the course of Coulomb collisions and their mixing due to the spin–orbital coupling.

The single-particle part $\hat{H}_0$ of the Hamiltonian $\hat{H}$ (we assume a simple parabolic conduction band structure) produces the diagonal terms in the matrix representation. The spin–orbit interaction, which we separate into the independent term $\hat{V}_{so}$, couples the charge- and spin-density wave excitation in the gas. Its form is discussed in detail in appendix A and, under conditions of the degeneracy of spin-split Landau levels, can be written as

$$\hat{V}_{so} = \sum_{n,p}\left(\sqrt{n+1}\frac{v_{so}(\hbar)\hbar}{\lambda_H}a^+_{n\uparrow p}a_{n+1\downarrow p} + \text{HC}\right). \tag{3}$$

The Coulomb interaction part of the Hamiltonian can be written in the usual way:

$$\begin{aligned}\hat{U} &= \frac{1}{2}\int \mathrm{d}x\ \mathrm{d}x'\ \hat{\psi}^+(x')\hat{\psi}^+(x)\frac{e^2}{\chi|x-x'|}\hat{\psi}(x)\hat{\psi}(x') \\ &= \frac{1}{2}\int \frac{\mathrm{d}q}{(2\pi)^2}\frac{2\pi e^2}{\chi q}[\hat{\rho}^+(q)\hat{\rho}(q) - \hat{\rho}(0)]\end{aligned} \tag{4}$$

where

$$\hat{\rho}(q) = \sum_{NN'p} F_{NN'}(q)\exp(\mathrm{i}q_y p)a^+_{Np}a_{N'p-q_x}$$

are Fourier components of the electron density operator, the coefficients

$$F_{NN'}(q) = \delta_{\alpha\alpha'}\sqrt{\frac{n'!}{n!}}\exp\left(-\frac{q^2+2\mathrm{i}q_xq_y}{4}\right)\left(\frac{\mathrm{i}q_y - q_x}{\sqrt{2}}\right)^{n-n'}L^{n-n'}_{n'}(\tfrac{1}{2}q^2)$$

come from the Fourier transform of the Landau wavefunction, $L^{n-n'}_{n'}$ are normalized generalized Laguerre polynomials (q is also dimensionless; see footnote on previous page) and χ is the effective dielectric constant of a media. To designate the intermediate stages of the calculations which give us the concrete form of the matrices in (2) we express the operator $\hat{\rho}(q)$ in (4) as

$$\hat{\rho}(q) = \sum_{N,N'} F_{NN'}(q)\hat{\Psi}^+_{NN'}(q).$$

We then use the algebra of excitonic operators and the fact that all Landau levels are either fully occupied or completely empty. These calculations can be also reformulated in diagrammatic language, and we refer the interested reader to earlier works [3, 15].

With the reduced matrix form of the Hamiltonian available, the calculation procedure is straightforward. The dispersion and internal structure of resulting charge- and spin-density excitations can be found after diagonalization of the matrices $H_{(\bar{N},\bar{N}')(NN')}(Q)$. The dispersion at $Q \to 0$ determines the frequencies of resonances, whereas the eigenfunctions combined of $\hat{\Psi}^+_{NN'}(Q)|0\rangle$ states help to analyse the optical activity of each transition. The dimension and specific form of the matrix Hamiltonian depend on the ground state of the system and on the set of excitons in resonance. We shall therefore consider its form for different filling factors separately.

3. CR–SR anticrossing at odd-integer filling factors

The set of basis excitons in resonance, and the form of the matrix Hamiltonian $H_{(\bar{N},\bar{N}')(NN')}(Q)$, are simpler in the case of odd-integer filling, $\nu = 2n+1$, when 2D electrons in the ground state completely fill both Landau levels, $(n+1, \downarrow)$ and $(n, \uparrow)$, with coincident energies.

From the point of view of the classification of low-lying excitations *the unit filling of the lowest Landau level* provides us with a clear example: there is a single magnetoplasma mode, $\omega_{\rm pl}(Q) = \omega_{\rm c} + Qe^2/2\hbar\chi$, in the system which is weakly coupled by the perturbation $\hat{V}_{\rm so}$ to a single spin $S = +1$ excitation, $\omega_{\rm s} + \xi Q^2$ [3,5]. This generates the 2×2 matrix to be diagonalized:

$$\hat{H} = \begin{pmatrix} \hbar\omega_{\rm c} & \hbar v_{\rm so}/\lambda_{\rm H} \\ \hbar v_{\rm so}/\lambda_{\rm H} & \hbar\omega_{\rm s} \end{pmatrix}.$$

(The plasmon group velocity can be approximated by $c/274\chi$, which is three orders of magnitude smaller than the speed of light, and which makes its dispersion negligible in the infrared absorption). Therefore, as shown in figure 1(*a*), the absorption peak near the crossing point $\omega_{\rm c} = \omega_{\rm s}$ is split by the spin–orbit coupling into two peaks

$$\omega_{\pm} = (\omega_{\rm c} + \omega_{\rm s})/2 \pm \sqrt{(\omega_{\rm c} - \omega_{\rm s})^2/4 + \delta_1^2}$$

of equal intensity. The splitting gap in this case is $2\delta_1$, where

$$\delta_1 = v_{\rm so}\lambda_{\rm H}^{-1} = p_{\rm F} v_{\rm so}(\hbar) \tag{5}$$

in complete agreement with the prediction of single-particle considerations [10]. In this estimation we used the magnetic field dependence of the spin–orbital coupling amplitude derived in appendix A, and the relation between the magnetic length and zero-field 2D Fermi momentum $p_{\rm F}$ in the gas.

At this point it is necessary to note that the observation of the splitting given by (5) can be expected in structures that are pure enough, provided that the Landau level broadening $\hbar\tau^{-1}$ (i.e. the CR linewidth) is less than the gap $\hbar v_{\rm so} p_{\rm F}$.

In the case of higher odd-integer filling there are four degenerate excitons near the crossing point. Two of them correspond to electron transitions between neighbouring Landau levels without any change of spin, but in interacting systems this does not mean the existence of two independent cyclotron resonances. The point is that the electromagnetic field can excite them only in the combination

$$A(Q)\hat{j}^{+}(Q) = e\lambda_{\rm H}\omega_{\rm c}(iA_y - A_x)\left(\sqrt{\frac{n+1}{2}}\hat{\Psi}^{+}_{(n+1)\downarrow n\downarrow}(Q) + \sqrt{\frac{n}{2}}\hat{\Psi}^{+}_{n\uparrow(n-1)\uparrow}(Q)\right) \tag{6}$$

which is just one of the eigenstates

$$\hat{\Psi}^{+}_{\rm pl} = \sqrt{\frac{n+1}{2n+1}}\hat{\Psi}^{+}_{n+1\downarrow n\downarrow}(Q) + \sqrt{\frac{n}{2n+1}}\hat{\Psi}^{+}_{n\uparrow n-1\uparrow}(Q)$$

of the corresponding block of the interaction Hamiltonian:

$$\hat{H}_{\rm int} = \frac{e^2}{\chi Q}\begin{pmatrix} |F_{(n+1)n}(Q)|^2 & F^{*}_{n(n-1)}(Q)F_{(n+1)n}(Q) \\ F_{n(n-1)}(Q)F^{*}_{(n+1)n}(Q) & |F_{n(n-1)}(Q)|^2 \end{pmatrix}$$

$$\simeq \frac{e^2}{\chi}Q\begin{pmatrix} n+1 & \sqrt{(n+1)n} \\ \sqrt{(n+1)n} & n \end{pmatrix}.$$

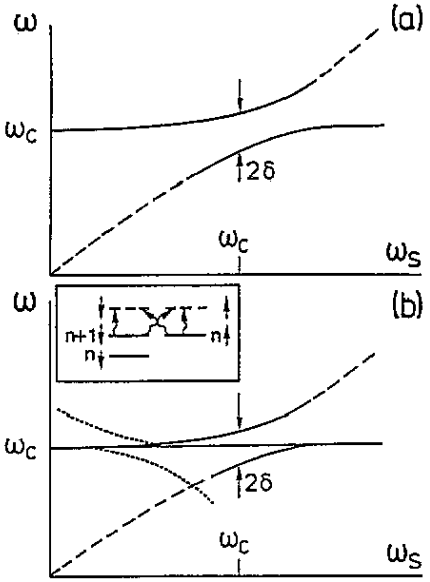

Figure 1. SR–CR line splitting near the crossing for filling factors (*a*) $\nu = 1$ and (*b*) $\nu = 3, 5 \ldots$ in the interacting electron gas. Full curves mark a transition with an intensity comparable to that of CR. Broken curves mark SR, and dots indicate the combined frequency resonance spectral position. The set of basic magneto-excitons is shown in the inset.

This 'optically active' mode has the linear dispersion

$$\omega_{\rm pl}(Q) = \omega_{\rm c} + \pi\sigma_{xy}Q/\chi$$

at small wavevectors and coincides directly with the classical magnetoplasma oscillations. The group velocity of such an excitation is exactly equal to

$$\partial\omega/\partial Q = \pi\sigma_{xy}/\chi.$$

Another mode

$$\hat{\Psi}^{+}_{\rm sd} = -\sqrt{\frac{n}{2n+1}}\hat{\Psi}^{+}_{n+1\downarrow n\downarrow}(Q) + \sqrt{\frac{n+1}{2n+1}}\hat{\Psi}^{+}_{n\uparrow n-1\uparrow}(Q)$$

can be treated like a spin-density wave with $S = 0$ and possesses a quadratic dispersion at $Q \to 0$ [3]. It is 'optically passive' and cannot be found in the CR experiments but, as we shall show below, it is simultaneously mixed with the spin $+1$ and magnetoplasma excitations in the vicinity of the CR–SR crossing.

We can now derive the magneto-exciton representation of the Hamiltonian in the form of a 4×4 matrix

$$\begin{pmatrix} \hbar\omega_{\rm c} + \frac{(2n+1)e^2}{2\chi}Q & 0 & \alpha^{*}_{\rm so}\frac{1}{\sqrt{2n+1}} & 0 \\ 0 & \hbar\omega_{\rm c} & -2\alpha^{*}_{\rm so}\sqrt{\frac{n(n+1)}{2n+1}} & \alpha_{\rm so}\sqrt{2n+1} \\ \alpha_{\rm so}\frac{1}{\sqrt{2n+1}} & -2\alpha_{\rm so}\sqrt{\frac{n(n+1)}{2n+1}} & \hbar\omega_{\rm s} & 0 \\ 0 & \alpha^{*}_{\rm so}\sqrt{2n+1} & 0 & \hbar(2\omega_{\rm c} - \omega_{\rm s}) + E^{\rm ex}_{-1} \end{pmatrix} \tag{7}$$

acting within the basis of states $(\hat{\Psi}^+_{\rm pl}, \hat{\Psi}^+_{\rm sd}, \hat{\Psi}^+_{+1}, \hat{\Psi}^+_{-1})|0\rangle$ (where $\hat{\Psi}^+_{+1}$ and $\hat{\Psi}^+_{-1}$ describe spin ± 1 excitons related to the spin (CR) and combined frequency (CFR) resonances, respectively).

The Hamiltonian in (7) contains all necessary information to analyse resonances near the crossing and study the efficiency of the electron–electron interaction effects. The latter manifest themselves in the shift of the energy of spin-1 mode

$$E^{\rm ex}_{-1} = \int \frac{{\rm d}q\ V(q)}{(2\pi)^2}\Bigg(\sum_{n_1<n}|F_{(n-1)n_1}(q)|^2 - \sum_{n_1\leqslant n}|F_{(n+1)n_1}(q)|^2 - F^*_{(n+1)(n+1)}(q)F_{(n-1)(n-1)}(q)\Bigg)$$

with respect to the single-particle energy $\hbar(2\omega_{\rm c} - \omega_{\rm s})$, which also means that the CR–SR and CR–CFR crossings take place at a different tilt of the magnetic field (this fact is schematically illustrated in figure 1(*b*)). As $E^{\rm ex}_{-1}$ is negative, (at $\nu = 3$, for instance, $E^{\rm ex}_{-1} = -\sqrt{\pi/2}\frac{3}{16}e^2/\chi\lambda_{\rm H}$) the crossing between CR and CFR occurs at $\omega_{\rm c} - \omega_{\rm s} = |E^{\rm ex}_{-1}/\hbar|$ and, if the spin–orbit coupling is much weaker than the Coulomb interaction, the 4×4 Hamiltonian should be replaced by simplified resonant 3×3 matrices, each deduced from (7) near one of the two resolved crossing points.

Near the CR–SR crossing the corresponding 3×3 matrix is given by the upper left block in (7). Its diagonalization leads to the algebraic equation

$$\delta\left(\delta^2 + (\omega_{\rm c} - \omega_{\rm s})\delta - (2n+1)\left|\frac{v_{\rm so}}{\lambda_{\rm H}}\right|^2\right) = (2n+1)\frac{e^2}{2\hbar\chi\lambda_{\rm H}}Q\left[\delta^2 + (\omega_{\rm c} - \omega_{\rm s})\delta - \left(2n+1-\frac{1}{2n+1}\right)\left|\frac{v_{\rm so}}{\lambda_{\rm H}}\right|^2\right] \tag{8}$$

on the resonance position counted off the cyclotron frequency value: $\omega = \omega_{\rm c} + \delta$. This equation can be easily solved in two limits: that of a high or of a negligibly small excitation momentum†. In most realistic systems the limit $Q < \omega_{\rm c}/c \to 0$ is an actual one. In this limit the right-hand side of (8) can be replaced by zero and then we find one mode with frequency $\omega_{\rm CR} = \omega_{\rm c}$ and relative intensity

$$I_{\rm CR} \propto 1 - 1/(2n+1)^2$$

and additional mixed modes with frequencies

$$\omega_\pm = \frac{\omega_{\rm c} + \omega_{\rm s}}{2} \pm \sqrt{\delta^2_{2n+1} + \left(\frac{\omega_{\rm c} - \omega_{\rm s}}{2}\right)^2} \qquad \delta_{2n+1} = \sqrt{2n+1}\,v_{\rm so}\lambda_{\rm H}^{-1}.$$

The relative intensities of the latter two modes are weak, and decrease rapidly when the Landau level number increases:

$$I_\pm \propto \frac{1}{2(2n+1)^2}\,\frac{1}{1+\Delta^2 \mp \Delta\sqrt{1+\Delta^2}}$$

† When $\pi\sigma_{xy}/\chi Q$ is much greater than the spin–orbit coupling, the resonant conditions are split once more, and the 3×3 matrix produces two 2×2 matrices which describe two independent crossings of the spin $(+1)$ mode with the magnetoplasmon and $S = 0$ spin-density wave, respectively. This means that only one of them can be found in the cyclotron resonance anomaly similar to that described for the unit filling, but with splitting $\delta = v_{\rm so}\lambda_{\rm H}^{-1}/\sqrt{2n+1}$. The splitting of $S = 0$ and $S = +1$ spin-wave excitations is much greater, $\delta = v_{\rm so}\lambda_{\rm H}^{-1}\sqrt{n(n+1)/(2n+1)}$, but is an internal event in the system and cannot be observed in absorption without the aid of impurities [17, 18].

where the parameter $\Delta = (\omega_c - \omega_s)/(2\sqrt{2n+1}v_{so}\lambda_H^{-1})$ shows how close to the crossing we are. In any case, the intensity of chipped satellite lines is maximal at lower filling factors and can be estimated as 5–10% of the main peak itself, whereas the characteristic splitting (the gap) which can be found after recalculation of the magnetic length at a fixed filling factor into the Fermi momentum in the gas at $H = 0$

$$\delta_{2n+1} = \sqrt{2n+1}\frac{v_{so}}{\lambda_H} = \sqrt{\frac{\nu}{\lambda_H^2}}v_{so} = p_F v_{so}(h) \tag{9}$$

is just equal to the zero magnetic field spin-splitting value [19], and has the same magnitude as at $\nu = 1$.

We now consider the CR–CFR crossing. The reduced 3×3 Hamiltonian related to this crossing can be obtained from (7) by excluding the matrix elements which correspond to the spin (+1) exciton. The optically active magnetoplasma mode is decoupled in this case, and the cyclotron resonance line should not change near its crossing with the CFR. The CFR mode mixes only with the optically passive spin-density wave $\hat{\Psi}_{sd}^{+}$ and does not produce any observable absorption anomaly at

$$\omega_c - \omega_s = |E_{-1}^{ex}|/\hbar.$$

The latter statement is specific to systems where the Coulomb effects are much stronger than the spin–orbit effects. As for systems where the spin–orbit interaction is dominant, active and passive modes can no longer be resolved because they are strongly intermixed through the spin-wave excitations (see (7)). The picture of the crossing of resonances transforms, therefore, into that obtained in the single-particle approximation [10].

4. Collective modes in the spin-polarized electron gas at even-integer filling factors

The analysis of even-integer filling factors is more complex since there is a choice of the system ground state under artificial degeneracy conditions. Compared to the previous case, the pair of degenerate Landau levels at $\nu = 2n + 2$ is 'half-filled', which gives some freedom to their repopulation and variation of the excitation wavefunctions on approaching the single-particle level crossing. From [11] we know that the exchange electron–electron interaction gives an earlier increase (at least at zero temperature) to the polarization in a 2D gas stimulated by the inter-Landau-level exchange (at $\omega_c > \omega_s$) than could be expected from a single-particle model. On the other hand, the spin–orbit repulsion of levels near the crossing tends to replace the phase transitions by a continuous mixing of states with opposite spins. As shown in appendix B, the crossover between these two characteristic behaviours takes place when

$$v_{so} \simeq \frac{3\sqrt{\pi}}{16\sqrt{2}}e^2/\chi\hbar$$

(this is an estimation for the filling factor two), and polarization transition always takes place while the spin–orbit coupling is weak. We shall therefore consider the spin–orbit coupling as a perturbation, analogously to what was done in the previous section, with the only difference being that the weak deformation of a ground state (introduced by $\hat{V}_{so}$) slightly

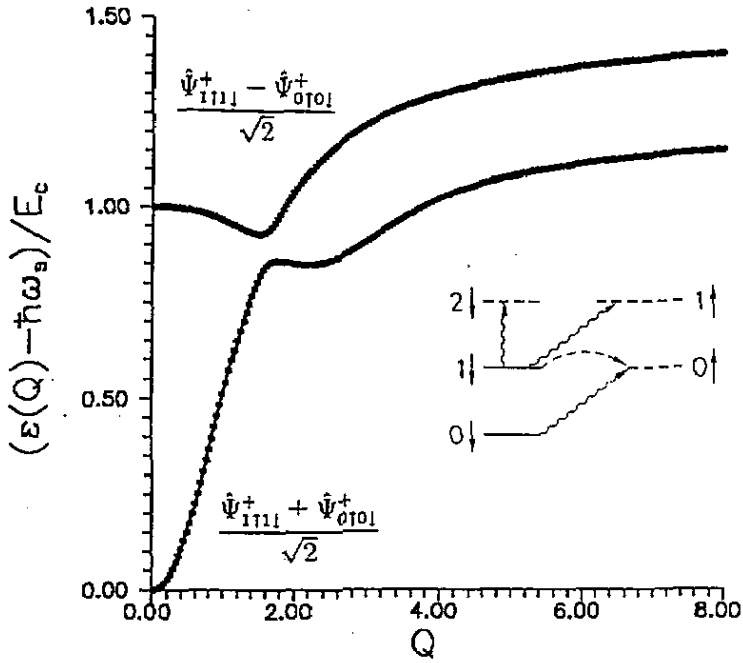

Figure 2. Energy dispersion of hybridized spin-density waves in the polarized state. The excitation energy is counted off the Zeeman splitting value and is normalized by $E_c = (\pi/2)^{1/2}e^2/\chi\lambda_H$; Q is the excitation momentum measured in units of inverse magnetic length λ_H^{-1}. The inset shows the primary basis of inter-Landau-level excitons in a spin-polarized state.

deforms single-particle creation and annihilation operators at coincident Landau levels. This correction is described in detail in appendix B and is insignificant for the crossing structure.

Therefore, in constructing the basic set of excitations in the aligned phase of 2D electrons (already stable at the crossing $\omega_c = \omega_s$) we can operate with unperturbed single-particle operators. For the sake of simplicity we first do our analysis for the filling factor $\nu = 2$. From the scheme of primary magneto-excitons shown in the inset to figure 2 one can find that, in addition to the single cyclotron mode $\hat{\Psi}^+_{2\downarrow1\downarrow}$ (it corresponds to $\hat{\Psi}^+_{2\downarrow\eta}$ in terms of operators corrected in appendix B), the polarized state has two spin-flip modes $\hat{\Psi}^+_{0\uparrow0\downarrow}$ and $\hat{\Psi}^+_{1\uparrow1\downarrow}$ related to the spin flip at different Landau levels (in appendix B these two are referred as $\hat{\Psi}^+_{\xi0\downarrow}$ and $\hat{\Psi}^+_{1\downarrow\eta}$). The block of the matrix Hamiltonian which describes them can be extracted as

$$\frac{1}{2}\sqrt{\frac{\pi}{2}}\frac{e^2}{\chi\lambda_H}\begin{pmatrix}1 & -1\\ -1 & 1\end{pmatrix} \tag{10}$$

and shows that the spin-density modes are hybridized into symmetric and antisymmetric combinations, $(\hat{\Psi}^+_{1\uparrow1\downarrow} \pm \hat{\Psi}^+_{0\uparrow0\downarrow})/\sqrt{2}$ (the single-particle energy $\hbar\omega_s$, equal for both of these combinations, is omitted in this equation).

Generally speaking, the symmetric mode describes the synchronous spin-flip for electrons at different ($n = 0$ and $n = 1$) Landau levels. Its frequency dispersion starts (at $Q = 0$) from the free-electron Zeeman splitting value, and this mode alone can be excited by an external alternative magnetic field in the SR experiment, which is in complete agreement with Larmor's theorem.

Another new antisymmetric branch of spin-density waves corresponds to the out-of-phase spin-flip at different Landau levels. In looking for an analogy, we can say that it is similar to the optical magnon in ferrimagnets with a complex unit cell. The dispersion curve of this excitation is shown in figure 2, and the energy gap (at $Q \to 0$) is sufficiently enhanced by the exchange Coulomb interaction with respect to the Zeeman splitting:

$$\epsilon(Q \to 0) = \hbar\omega_s + E_c - AQ^2$$

where

$$E_c = \sqrt{\frac{\pi}{2}}\, e^2/\chi\lambda_H.$$

Although this mode cannot be excited in an ordinary spin resonance experiment, its existence nevertheless influences the CR fine structure near the crossing point.

5. CR–SR anticrossing in the spin-polarized phase

The latter expectation arises from the fact (clear from the inset in figure 2) that only the $\hat{\Psi}^+_{1\uparrow 1\downarrow}$ spin-exciton from the primary basis can be coupled by the interaction $\hat{V}_{so}$ to the magnetoplasma mode $\hat{\Psi}^+_{2\downarrow 1\downarrow}$. This means that, after hybridization, the first-order spin–orbit interaction (whose amplitude is equal to $\sqrt{2}\hbar v_{so}/\lambda_H$) should be 'equally redistributed' between two symmetrized modes $(\hat{\Psi}^+_{1\uparrow 1\downarrow} \pm \hat{\Psi}^+_{0\uparrow 0\downarrow})/\sqrt{2}$. The relevant block of the matrix Hamiltonian can therefore be written in the form

$$\begin{pmatrix} \hbar\omega_c & \frac{\hbar v_{so}}{\lambda_H} & \frac{\hbar v_{so}}{\lambda_H}(1+\gamma) & 0 \\ \frac{\hbar v_{so}}{\lambda_H} & \hbar\omega_s & 0 & 0 \\ \frac{\hbar v_{so}}{\lambda_H}(1+\gamma) & 0 & \hbar\omega_s + E_c & H_{12} \\ 0 & 0 & H_{12}^+ & H_{22} \end{pmatrix} \tag{11}$$

where

$$\gamma = \frac{\sqrt{2}}{4}\frac{E_c}{\frac{3}{4}E_c + \omega_s - \omega_c}$$

accounts for the effect of spin–orbital coupling on the ground state of the system, i.e. the deviation of exact operators $\hat{\Psi}^+_{\xi(0\downarrow)}$ and $\hat{\Psi}^+_{(1\uparrow)\eta}$ determined in appendix B from the primary basis of excitons $\hat{\Psi}^+_{0\uparrow 0\downarrow}$ and $\hat{\Psi}^+_{1\uparrow 1\downarrow}$. As above,

$$E_c = \sqrt{\frac{\pi}{2}}\, e^2/\chi\lambda_H.$$

The term H_{12} describes the decay of the antisymmetric spin-density wave $(\hat{\Psi}^+_{1\uparrow 1\downarrow} - \hat{\Psi}^+_{0\uparrow 0\downarrow})/\sqrt{2}$ into a continuum of two-electron excitations composed of pairs of cyclotron $(\hat{\Psi}^+_{2\downarrow 1\downarrow})$ and spin +1 low-energy $(\hat{\Psi}^+_{0\uparrow 1\downarrow})$ excitons. After symmetrization the mode $(\hat{\Psi}^+_{1\uparrow 1\downarrow} + \hat{\Psi}^+_{0\uparrow 0\downarrow})/\sqrt{2}$ does not interact with the continuum spectrum, which fits reasonably to Larmor's theorem. Moreover, turning to the Hartree–Fock procedure in appendix B, we

should omit the 'spontaneous' creation of $\hat{\Psi}^{+}_{0\uparrow 1\downarrow}$ excitons (more accurately, after the ground-state deformation by the spin–orbit term $\hat{V}_{so}$ this is the exciton $\hat{\Psi}^{+}_{\xi\eta}$), the cyclotron mode is thus decoupled from the two-excitonic states (at least in the first order on the spin–orbit interaction) and one can find from (11) that these two resonances near the crossing are split into two lines with equal intensities and separated by the gap $2\delta_2$.

At this point we should emphasize that the sufficient off-diagonal spin–orbit term in Hamiltonian (11) is suppressed by a factor $1/\sqrt{2}$ compared to those in (3) for the first pair of empty Landau levels at $\nu = 2$. This statement becomes more obvious if we take into account the relation between λ_H and zero magnetic field Fermi momentum p_F for fixed $\nu = 2\pi n_e \lambda_H$, and find that $\delta_2 = p_F v_{so}/\sqrt{2}$. This seems to be an exclusive indirect spectral indication of the antisymmetric exciton in infrared absorption and the only possibility to observe this mode in CR experiments, because its imaginary crossing with the magnetoplasmon in (11) occurs in the instability region of a polarized phase.

In extending our analysis to the polarized state at higher even-integer filling factors, we should consider one additional inter-Landau-level transition mode $\hat{\Psi}^{+}_{n\uparrow(n-1)\uparrow}$ in the basis set of excitons. This increases the matrix Hamiltonian dimension, but the appropriate choice of magnetoplasma and $S = 0$ spin-density wave already mentioned in section 3 reduces the problem to that considered above. That is, the CR line acquires in the vicinity of the crossing two weak satellites, similar to those in figure 1(*b*), whereas the imaginary crossing of magnetoplasma modes $\hat{\Psi}_{pl}$ and $\hat{\Psi}_{sd}$ with an antisymmetric spin +1 exciton can be ignored because it occurs in the region of polarization instability. Therefore the only (if nevertheless important) difference from the picture of the odd-integer filling consists in the $1/\sqrt{2}$ reduction of the gaps between the three optically active modes:

$$\omega_{CR} = \omega_c \qquad \omega_{\pm} = \frac{\omega_c + \omega_s}{2} \pm \sqrt{\left(\frac{\omega_c - \omega_s}{2}\right)^2 + \delta^2_{2n+2}}$$

where

$$\delta_{2n+2} = \sqrt{\frac{\nu}{2}}\frac{v_{so}}{\lambda_H} = \frac{p_F v_{so}(h)}{\sqrt{2}} \tag{12}$$

in comparison with $\delta_{2n+1} = p_F v_{so}$ for a non-polarized gas at $\nu = 2n + 1$.

As for the non-polarized state at $\nu = 2n + 2$, we do not expect any CR–SR line crossing in this case because the full occupation of the $(n\uparrow)$ state forbids the spin-flip $S = 1$ transition. Therefore only CR–CFR crossing is meaningful. At $\nu = 2$, this crossing occurs at $\omega_c - \omega_s = \frac{1}{4}E_c$, where the non-polarized phase is completely unstable. For higher filling one can expect two coupled CFR modes and, after some hybridization, find that one of them lies in the region where the ground state can be non-polarized. Nevertheless, as follows from our consideration in section 3, the CFR mode can be only mixed with the optically passive mode $\hat{\Psi}^{+}_{sd}$; hence the CR is insensitive to this crossing.

6. Summary: Shubnikov–de Haas oscillations of the CR fine structure

Although the above consideration is related to the integer filling factors, where the excitonic representation works rigorously, the comparison of the Coulomb gas results with those for a single-particle model [10] leads us to believe that the most pronounced changes with the CR line-shape (for a tilting angle which provides the crossing conditions, $\omega_s = \omega_c$) takes

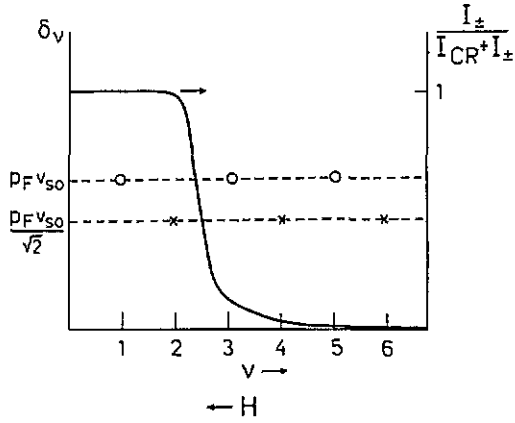

Figure 3. Relative intensity of chipped lines as a function of a filling factor (the spline is made by eye). Crosses and circles mark the spin–orbital gaps in the CR fine structure for odd-integer filling factors and even-integer filling factors, respectively.

place between the filling factors $\nu = 1$ and $\nu = 3$. At $\nu < 2$ the crossing seems to manifest itself in two lines split into $\delta = v_{so}/\lambda_H$ (figure 1(*a*)), whereas at $\nu > 3$ the absorption line is composed of a huge peak placed just at the unperturbed CR frequency $\omega_{CR} = \omega_c(H_z)$ and of two chipped weak satellites (figure 1(*b*)). The simplest scenario for this transition can, therefore, be viewed as the appearance of an unperturbed CR peak at $\nu = 2$ whose intensity I_{CR} increases with the filling up to 90% at $\nu = 3$, whereas the split lines (intensive at the lowest filling) become weak satellites, as shown in figure 3. The gaps separating these additional resonances are of the order of the magnitude of the zero magnetic field spin splitting and take the value of $v_{so}p_F$ at odd-integer filling factors and $v_{so}p_F/\sqrt{2}$ at even-integer filling factors. The scale of the splitting is independent of the specific value of an applied field: it is fixed by the areal density of 2D electrons. This allows us to present the idea of direct measurements of the spin–orbit coupling in heterostructures. Furthermore, the new kind of Shubnikov–de Haas oscillations in the CR fine structure results from the re-entrance of the 2D system into a partially spin-polarized state expected at even filling in a sufficiently tilted magnetic field, and can be an indication of a specific spin-density wave mode in it. We therefore propose a method of spectroscopical observation of the spin-polarization phase transition in the 2D electronic system at sufficiently tilted magnetic fields.

Acknowledgments

The author is grateful to K Efetov, R Haug, K von Klitzing, L Levy, A MacDonald and M Potemski for stimulating discussions. The support of the Alexander von Humboldt Foundation is acknowledged, and the author also wishes to acknowledge a NATO Collaborative Research Grant 921333 for providing the possibility to discuss this work with colleagues from HMFL-MPI.

Appendix A. Effective spin–orbit coupling between degenerate Landau levels

The aim of this appendix is to discuss the spin–orbit coupling in 2D electron gas in

heterostructures and to describe how of the term $\hat{V}_{so}$ in the secondary quantized Hamiltonian in (2) is derived. To be consistent with previous theories [20–22], we start the analysis with the 3D spin–orbit term in the conduction band electron dispersion, which for zinc blende-type semiconductors (like GaAs, InP, InAs) is known in the form

$$H_{so} = 2\alpha s\boldsymbol{K}(\boldsymbol{p}) + 2\beta s(\boldsymbol{p} \times \boldsymbol{E}) \tag{A1}$$

where

$$K_x(\boldsymbol{p}) = \{p_x, (p_y^2 - p_z^2)\}$$
$$K_y(\boldsymbol{p}) = \{p_y, (p_z^2 - p_x^2)\}$$
$$K_z(\boldsymbol{p}) = \{p_z, (p_x^2 - p_y^2)\}.$$

The brackets denote the anticommutation $\{a, b\} = (ab + ba)/2$, and $\boldsymbol{p} = -i\hbar\nabla - e\boldsymbol{A}/c$ is the momentum operator in a magnetic field. The first term in this equation results from the intrinsic lack of inversion symmetry in the bulk material. The second is caused by an electric field built into the heterojunction.

To get an expression for the effective 2D spin–orbit coupling related to the lowest size-quantized subband, we retain in (A1) only terms containing p_z^2 and then derive the 2D spin–orbital coupling which is linear in p_x and p_y. Depending on the internal symmetry of the heterostructure it can be composed of two parts:

$$H_{so}^{(2D)} = 2A(s_y p_y - s_x p_x) + 2Bs(\boldsymbol{p}_{\|} \times \boldsymbol{l}_z). \tag{A2}$$

One part is specific to the planar symmetry of a square lattice with the lack of an inversion centre and is allowed, for example, in structures grown along the axis (100) ($A = \alpha\langle p_z^2\rangle$ and $B = \beta\langle E_z\rangle$). The other part, proposed by Bychkov and Rashba [22], is axially symmetrical and is only possible in junctions grown along the axis (111), because their intrinsic symmetry is that of a triangular lattice. Because these two terms are of a different symmetry, the electron states at a zero magnetic field can be classified by their spin projection onto some axis $\boldsymbol{l}_p$, which can be found from the direction of the electron momentum with respect to the lattice axes. At $H = 0$, the states $s\boldsymbol{l}_p = \pm 1/2$ are split, and it is convenient to introduce the following quantity: the effective 2D spin–orbital velocity $v_{so}(\boldsymbol{p}/p)$ which varies with the momentum rotation with respect to the crytallographic axes. Near the Fermi level, this gives us the value of the so-called zero magnetic field spin splitting $p_F v_{so}$ [19, 23, 24].

Turning to the case of a quantizing magnetic field, we choose a gauge

$$\boldsymbol{A} = (-H_z y + H_y z, -H_x z, 0)$$

and a representation

$$p_x = -(\hat{b} + \hat{b}^+)\hbar/\lambda_H\sqrt{2} \qquad p_y = i(\hat{b}^+ - \hat{b})\hbar/\lambda_H\sqrt{2}$$

of the electron momentum in terms of 'creation' ($\hat{b}^+$) and 'annihilation' ($\hat{b}$) operators acting in the space of Landau wavefunctions ($\psi_n = \hat{b}^+\psi_{n-1}/\sqrt{n} = \hat{b}\psi_{n+1}/\sqrt{n+1}$, $\hat{b}\hat{b}^+ - \hat{b}^+\hat{b} = 1$). When the size quantization dominates the cyclotron rotation around the tilted magnetic field, we can neglect the influence of a parallel magnetic field component on the electronic subbands and arrive

$$H_{so} = \frac{A\hbar}{\lambda_H\sqrt{2}}\hat{b}u\{2s_h R_h + s_+ R_+ + s_- R_-\} + \text{HC}.$$

In this expression $h_\parallel = \sqrt{1-h_z^2}$, $u = (h_x - \mathrm{i}h_y)/h_\parallel$, $R_h = h_\parallel(1 - \mathrm{i}\rho/u^2)$, $R_\pm = \mp u^{\pm 1}[(1 \mp h_z) + \mathrm{i}\rho(1 \pm h_z)/u^2]$ and $\rho = B/A$. As to the spin, we choose the axis $\boldsymbol{h} = \boldsymbol{H}/H$ for its projection s_h and

$$s_+ = \begin{pmatrix} 0 & 1 \\ 0 & 0 \end{pmatrix} \qquad s_- = \begin{pmatrix} 0 & 0 \\ 1 & 0 \end{pmatrix}$$

are defined as s_h-increasing and s_h-decreasing operators, respectively.

Under crossing conditions we do not need the complete form of coupling in (A2) but extract only the term relating the pairs of degenerate Landau levels. This gives us the desired spin–orbit part of the Hamiltonian in the secondary quantized representation:

$$\hat{V}_{\mathrm{so}} = \sum_{n,p}\left(\sqrt{n+1}\,\frac{v_{\mathrm{so}}\hbar}{\lambda_{\mathrm{H}}}a^+_{n+1\downarrow p}a_{n\uparrow p} + \mathrm{HC}\right)$$

where

$$v_{\mathrm{so}}(\hbar) = \frac{A}{\sqrt{2}}\sqrt{(1 - gh_z/|g|)^2 - 4h_xh_y\rho + \rho^2(1 + gh_z/|g|)^2} \tag{A3}$$

is slightly modulated depending on the magnetic field orientation in the plane of 2D gas relative to the crystallographic axes†.

Appendix B. Polarization phase transition in the presence of the spin–orbit coupling

In this appendix we give an extension of a theory [11] to systems with a pronounced spin–orbit coupling. That is, we analyse the competition between the exchange Coulomb interaction and spin–orbit coupling effects on the gas ground-state formation and determine appropriate single-particle operators in order to construct excitons in a slightly deformed polarized state.

Following [11], we apply the Hartree–Fock approximation and use the method of Bogolubov–Valatin transformations. That is, the Fermi-operators of electrons at two crossing Landau levels $N = (n+1, \downarrow)$ and $N' = (n, \uparrow)$ should be mixed by a unitary rotation

$$\hat{a}_{Np} = x\hat{\eta}_p + y\hat{\xi}_p \qquad \hat{a}_{N'p} = -y\hat{\eta}_p + x\hat{\xi}_p \qquad |x|^2 + |y|^2 = 1$$

so that the ground state $|0\rangle$ of the system has some completely filled 'level' η, $\langle 0|\hat{\Psi}_{\eta\eta}(0)|0\rangle = S$, and another completely empty 'level' ξ, $\hat{\xi}|0\rangle = 0$ (S is an area of a system which is, in fact, the normalization factor omitted everywhere above). The complex parameters x and y can be found by minimizing the corresponding part of the ground-state energy:

$$\begin{aligned} E_0(x,y) = \langle 0|\hat{H}|0\rangle &= -\hbar(\omega_{\mathrm{c}} - \omega_{\mathrm{s}})|y|^2 - \sqrt{n+1}\,\frac{\hbar v_{\mathrm{so}}}{\lambda_{\mathrm{H}}}(xy^* + x^*y) \\ &+ \frac{1}{2}\int \frac{\mathrm{d}q\; V(q)}{(2\pi)^2}\left(\sum_{N_i > N,N'}(|x|^2|F_{N_iN}|^2 + |y|^2|F_{N_iN'}|^2)\right) \\ &+ \left(\sum_{N_i < N,N'}(|y|^2|F_{NN_i}|^2 + |x|^2|F_{N'N_i}|^2) - 1 + |xy^*F_{NN} - yx^*F_{N'N'}|^2\right) \end{aligned} \tag{B1}$$

† One detail which can be important for experimental studies in realistic systems is the following. When a tilted magnetic field is strong, it can destroy the separation of in- and across-plane variables. In this extreme limit one can represent the electron wavefunctions in the form of size-quantized states $|m\rangle$ along the magnetic field direction based on the lowest 3D Landau level [25]. After neglecting the electric-field induced term, we can get the spin–orbital splitting gap $(3\hbar^2|\alpha|/\lambda_{\mathrm{H}}^2)\,|\langle m+1|p_h|m\rangle|\,|h_xh_y|$, where $\lambda_{\mathrm{H}} = (eH/\hbar c)^{1/2}$. Compared to the purely 2D case, this gap depends on the magnetic field orientation in the plane and varies from the maximal value realized for $\boldsymbol{H}_\parallel$ oriented at (011) directions, to almost zero at (010) or (001).

with the normalization conditions

$$\sum_{N_i} |F_{N_i N}(q)|^2 = 1 \qquad |x|^2 + |y|^2 = 1$$

to be taken into account.

This algebra leads us to some more clear expression for the ground-state energy:

$$E_0(x, y) = |y|^2 \Bigg[\omega_s - \omega_c + \frac{1}{2} \int \frac{dq\, e^2}{2\pi\chi q} \Bigg(\sum_{n_1=0}^{n-1} 2(|F_{n_1(n+1)}|^2 - |F_{n_1 n}|^2) + 2|F_{n(n+1)}|^2 + |F_{(n+1)(n+1)}|^2 - |F_{nn}|^2 \Bigg) \Bigg] - 2\sqrt{n+1}|\alpha_{so}|\sqrt{|y|^2(1-|y|^2)} + |y|^2(1-|y|^2) \times \frac{1}{2} \int \frac{dq\, e^2}{2\pi\chi q} |F_{(n+1)(n+1)} - F_{nn}|^2. \tag{B2}$$

Equation (B2) shows that if

$$\frac{\hbar v_{so}}{\lambda_H} < \frac{1}{4\sqrt{2(n+1)}} \frac{e^2}{\chi\lambda_H} \int \frac{dz}{\sqrt{z}} e^{-z} |L^0_{n+1}(z) - L^0_n(z)|^2 \tag{B3}$$

the polarization undergoes a jump (i.e. a phase transition) when the expression in the first bracket in (B1) is equal to zero (i.e. at $\omega_c > \omega_s$), and changes continuously (no phase transition at all) when the inequality opposite to that in (B3) takes place. For the lowest filling $\nu = 2$, the relevant constant is

$$\hbar v_{so} \lambda_H^{-1} \simeq \tfrac{3}{16} E_c \qquad E_c = \sqrt{\pi/2}(e^2/\chi\lambda_H)$$

which requires too high an effective 2D spin–orbital velocity, $v_{so} \sim 4 \times 10^6\,\mathrm{cm\,s^{-1}}$, for it to be the dominant spin–orbit effect (in most wide band gap materials $v_{so} < 10^6\,\mathrm{cm\,s^{-1}}$ [20]). We can thus look upon the effect of spin–orbit coupling as being weak in comparison with the Coulomb interaction, so that our system chooses the ground state to be either polarized, or non-polarized, and the Bogolubov–Valatin transformation mixes the N and N' levels only slightly.

This slight deformation of the polarized state at $\nu = 2$ ($x \to 1$) is described by the Bogolubov–Valatin transformation coefficient

$$y \sim v_{so}\lambda_H^{-1}/(\tfrac{3}{4}E_c + \omega_s - \omega_c).$$

(In the non-polarized phase ($x \to 0$) the mixing of spin-up and spin-down operators is given by $x \sim v_{so}\lambda_H^{-1}/(\omega_c - \omega_s)$). This strictly determines new single-particle creation (annihilation) operators $\hat{\xi}$ and $\hat{\eta}$, and allows us to define the correct excitonic wavefunctions $\hat{\Psi}^+_{n+1\downarrow,\eta}$, $\hat{\Psi}^+_{\xi,n-1\uparrow}$, $\hat{\Psi}^+_{\xi,n\downarrow}$, $\hat{\Psi}^+_{n+1\uparrow\eta}$ analogously to section 3. In the polarized phase,

$$\hat{\Psi}^+_{n+1\downarrow,\eta} \simeq \hat{\Psi}^+_{n+1\downarrow n+2\downarrow} \qquad \hat{\Psi}^+_{\xi,n-1\uparrow} \simeq \hat{\Psi}^+_{n\uparrow n-1\uparrow}$$

describe the inter-Landau-level transitions participating in the CR formation; and

$$\hat{\Psi}^+_{\xi,n\downarrow} \simeq \hat{\Psi}^+_{n\uparrow n\downarrow} \qquad \hat{\Psi}^+_{n+1\uparrow\eta} \simeq \hat{\Psi}^+_{n+1\uparrow n+1\downarrow}$$

are related to the spin-flip transitions and form the spin-density waves. Finally, the lowest-energy exciton $\hat{\Psi}^+_{\xi\eta}$ corresponds to the inter-Landau-level spin-1 mode.

As well as the first-order transition point $\omega_c - \omega_s = \frac{3}{8}E_c$ (this is an estimate [11] for $\nu = 2$), each phase has a point of complete instability. In the polarized state the instability develops at $\omega_c - \omega_s = \frac{3}{4}E_c$. The non-polarized state is completely unstable at $\omega_c < \omega_s$.

References

[1] Kohn W 1961 *Phys. Rev.* **123** 1242
[2] Horing N and Yildiz M 1976 *Ann. Phys., NY* **97** 216
[3] Kallin C and Halperin B I 1984 *Phys. Rev.* B **30** 5655
[4] Janak J F 1969 *Phys. Rev.* **178** 1416
[5] Bychkov Yu A, Iordanskii S V and Eliashberg G M 1981 *Pis. Zh. Eksp. Teor. Fiz.* **33** 152 (Engl. Transl. 1981 *JETP Lett.* **33** 143)
Bychkov Yu A and Rashba E I 1983 *Zh. Eksp. Teor. Fiz.* **85** 1826 (Engl. Transl. 1983 *Sov. Phys.–JETP* **58** 1062)
[6] Dobers M, von Klitzing K and Weimann G 1988 *Phys. Rev.* B **38** 5453
[7] Takada Y and Ando T 1978 *J. Phys. Soc. Japan* **44** 905
[8] Appel J and Overhauser A W 1978 *Phys. Rev.* B **18** 758
[9] MacDonald A H and Kallin C 1989 *Phys. Rev.* B **40** 5795
[10] Fal'ko V I 1992 *Phys. Rev.* B **46** 4320
[11] Guiliani G F and Quinn J J 1985 *Phys. Rev.* B **31** 6228
[12] Nicholas R J, Haug R J, von Klitzing K and Weimann G 1988 *Phys. Rev.* B **37** 1294
[13] Koch S, Haug R J, von Klitzing K and Razeghi M 1993 *Phys. Rev.* B **47** 4048
[14] Fal'ko V I 1993 *Phys. Rev. Lett.* **71** 141
[15] Lerner I V and Losovik Yu E 1980 *Zh. Eksp. Teor. Fiz.* **78** 1167 (Engl. Transl. 1980 *Sov. Phys.–JETP* **51** 588)
[16] Janovici B 1981 *Phys. Rev. Lett.* **46** 386
[17] Kallin C and Halperin B I 1985 *Phys. Rev.* B **31** 3635
[18] Wu J-W, Hawrylak P and Quinn J J 1985 *Phys. Rev.* B **31** 6592
[19] Lommer G, Malcher F and Rossler U 1988 *Phys. Rev. Lett.* **60** 728
[20] Malcher F, Lommer G and Rossler U 1986 *Superlatt. Microstruct.* **2** 273
Rashba E I and Sherman E Yu 1988 *Phys. Lett.* **129A** 175
Lommer G, Malcher F and Rossler U 1988 *Phys. Rev. Lett.* **60** 729
Pfeffer P and Zawadski W 1990 *Phys. Rev.* B **41** 1561
[21] Dresselhaus G 1955 *Phys. Rev.* **100** 580
Bir G L and Pikus G E 1974 *Symmetry and Strain Induced Effects in Semiconductors* (New York: Wiley)
Pfeffer P and Zawadskii W 1990 *Phys. Rev.* B **41** 1561
[22] Bychkov Yu A and Rashba E I 1984 *Sov. Phys.–JETP Lett.* **39** 78
Rashba E I and Sheka V I 1991 *Landau Level Spectroscopy (Modern Problems in Condensed Matter Science 133)* ed G Landwehr and E I Rashba (Amsterdam: Elsevier)
[23] Luo J, Munekata H, Fang F F and Stibes P J 1988 *Phys. Rev.* B **38** 10142
Das B, Miller D C, Datta S, Reifenberger R, Hong W P, Bhattacharya B K, Singh J and Jaffe M 1989 *Phys. Rev.* B **39** 1411
Das B, Datta S and Reifenberger R 1990 *Phys. Rev.* B **41** 8278
[24] Jusserand B, Richards B, Peric H and Etienne B 1992 *Phys. Rev. Lett.* **69** 848
[25] Fal'ko V I 1991 *Solid State Commun.* **78** 925
Kirpichev V E, Kukushkin I V, Timofeev V B and Fal'ko V I 1990 *Sov. Phys.–JETP Lett.* **51** 436
Kutter M C, Maan J C, Chitta V, Fal'ko V I, Eaves L and Heinini M 1992 *Phys. Rev.* B **45** 8748